

Hysteresis and unusual magnetic properties in the singular Heusler alloy Ni₄₅Co₅Mn₄₀Sn₁₀

Vijay Srivastava, Xian Chen, and Richard D. James

Citation: *Applied Physics Letters* **97**, 014101 (2010); doi: 10.1063/1.3456562

View online: <http://dx.doi.org/10.1063/1.3456562>

View Table of Contents: <http://scitation.aip.org/content/aip/journal/apl/97/1?ver=pdfcov>

Published by the [AIP Publishing](#)

Articles you may be interested in

[Tuning the magnetocaloric properties of the Ni_{2+x}Mn_{1-x}Sn Heusler alloys](#)

J. Appl. Phys. **113**, 173911 (2013); 10.1063/1.4803860

[Concentration dependence of magnetic moment in Ni_{50-x}Co_xMn_{50-y}Z_y \(Z = In, Sn\) Heusler alloys](#)

Appl. Phys. Lett. **97**, 242512 (2010); 10.1063/1.3525168

[The martensitic transformation, magnetocaloric effect, and magnetoresistance in high-Mn content Mn_{47+x}Ni_{43-x}Sn₁₀ ferromagnetic shape memory alloys](#)

J. Appl. Phys. **108**, 103920 (2010); 10.1063/1.3511748

[Magnetic properties and magnetocaloric effect of \(Mn_{1-x}Ni_x\)₃Sn₂ \(x = 0 – 0.5\) compounds](#)

J. Appl. Phys. **105**, 07A935 (2009); 10.1063/1.3062953

[Magnetocaloric properties of Mn₃Sn₂ from heat capacity measurements](#)

J. Appl. Phys. **105**, 033905 (2009); 10.1063/1.3074093



AIP | Journal of
Applied Physics

Journal of Applied Physics is pleased to
announce **André Anders** as its new Editor-in-Chief

Hysteresis and unusual magnetic properties in the singular Heusler alloy $\text{Ni}_{45}\text{Co}_5\text{Mn}_{40}\text{Sn}_{10}$

Vijay Srivastava, Xian Chen, and Richard D. James^{a)}

Department of Aerospace Engineering and Mechanics, 107 Akerman Hall, University of Minnesota, Minneapolis, Minnesota 55455, USA

(Received 25 April 2010; accepted 3 June 2010; published online 6 July 2010)

The alloy $\text{Ni}_{45}\text{Co}_5\text{Mn}_{40}\text{Sn}_{10}$ is shown to be singular relative to nearby alloys in three following ways: (1) The austenite has remarkably high magnetization (1170 emu/cm^3) and low magnetic anisotropy. (2) The thermal hysteresis is near minimum. (3) The transformation temperature $\sim 135^\circ\text{C}$ is unusually high. Because the unusually large magnetization and low hysteresis is seen at relatively small applied fields, applications such as magnetic shape memory, energy conversion, and solid state refrigeration may become practical. © 2010 American Institute of Physics.
[doi:10.1063/1.3456562]

An attractive strategy for the discovery of new materials is to combine a big first order phase transformation and interesting electromagnetic properties.¹ The change in lattice parameters at transformation, together with the lattice-parameter-sensitivity of electromagnetic properties, suggests the two phases can have diverse properties. While such phase transformations are sometimes not reversible, there is increasing evidence that certain conditions for low hysteresis¹⁻⁴ promote cyclic reversibility. The alloy $\text{Ni}_{45}\text{Co}_5\text{Mn}_{40}\text{Sn}_{10}$, with nonferromagnetic martensite and ferromagnetic austenite, was found using this strategy.

Because of their propensity toward ferromagnetism and the abundance of martensitic phase transformations, Heusler alloys provide attractive starting points for this strategy. Beginning with the Ni_2MnGa martensitic-ferromagnetic alloy (Webster *et al.*⁵), a large number of Heuslers with phase transformations have been studied. Of particular relevance to the present study are the NiMnX alloys, $X=\text{In, Sn, and Sb}$,^{6,7} which have a martensitic transition from a weakly ferromagnetic martensite phase [In this paper, M_s denotes the martensite start temperature and m_s denotes the saturation magnetization.] ($m_s \sim 40\text{--}80 \text{ emu/cm}^3$) to a moderately ferromagnetic austenite phase ($m_s \sim 150\text{--}200 \text{ emu/cm}^3$). As shown by Kainuma *et al.*⁸ (also Ref. 9), substitutions of Co for Ni increase m_s . For example, $\text{Ni}_{43}\text{Co}_7\text{Mn}_{39}\text{Sn}_{11}$ exhibits $m_s \sim 640 \text{ emu/cm}^3$ at 4 T, while $\text{Ni}_{45}\text{Co}_5\text{Mn}_{36.6}\text{In}_{13.4}$ shows $m_s \sim 800 \text{ emu/cm}^3$ at 7 T.^{10,11} Exceptionally low thermal hysteresis is seen¹² in the magnetization versus temperature curves in the alloy $\text{Ni}_{47}\text{Co}_3\text{Mn}_{37}\text{Sn}_{13}$ at fields of 5 T.

The conditions for low thermal hysteresis and reversibility that guide our compositional changes are described elsewhere.¹⁻³ The particular condition used here is $\lambda_2=1$, where λ_2 is the middle eigenvalue of the transformation stretch matrix. A growing body of work establishes a significant relation between $\lambda_2=1$ and hysteresis. For example, in a recent study of alloys of TiNiCuPd by Zarnetta *et al.*⁴ it is found that the thermal hysteresis drops precipitously from about 70°C to near zero as $\lambda_2 \rightarrow 1$, and this is accompanied by an improvement of the alloy stability under repeated transformation. The condition $\lambda_2=1$ is a necessary and sufficient condition that there exists an unstressed, untwinned

interface between the phases. Recent theoretical work³ correlates the presence of this kind of interface with a dramatic decrease in the energy barrier accompanying the growth of the incipient phase. Following work of Krenke *et al.*,¹³ our starting point was the basic system $\text{Ni}_{50}\text{Mn}_{50-x}\text{Sn}_x$, which shows low thermal hysteresis at $x=10$. We determined from x-ray measurements that λ_2 was slightly greater than 1 in $\text{Ni}_{50}\text{Mn}_{40}\text{Sn}_{10}$ and increases strongly with x .¹⁴ We thus decreased the Sn content and achieved $\lambda_2=1$ and minimum hysteresis at about $x=9$, at which composition the hysteresis decreased to about 6°C by our differential scanning calorimetry (DSC) measurement. From compositions near this minimum hysteresis alloy we substituted Co for Ni, and used the goal $\lambda_2=1$, to arrive at the present alloy. Our experimental methods are described in detail in Ref. 3. Figure 1 shows DSC curves for $\text{Ni}_{45}\text{Co}_5\text{Mn}_{40}\text{Sn}_{10}$. Both forward and reverse martensitic transitions are accompanied by well-defined peaks, arising from the latent heat of the transformation. The temperatures for the forward and reverse transformation are denoted A_s (austenite start), A_f (austenite finish), M_s (martensite start), and M_f (martensite finish). The formula $A_f - M_s$ is used to calculate the thermal hysteresis and this is found to be 6°C . This was the lowest value of hysteresis found among the alloys $\text{Ni}_{50}\text{Mn}_{50-x}\text{X}_x$ ($X=\text{Sn, In; } x=9, 10, 11, 12, 13$ and $\text{Ni}_{50-x}\text{Co}_x\text{Mn}_{40}\text{Sn}_{10}$; $x=3, 5, 7, 9$, the

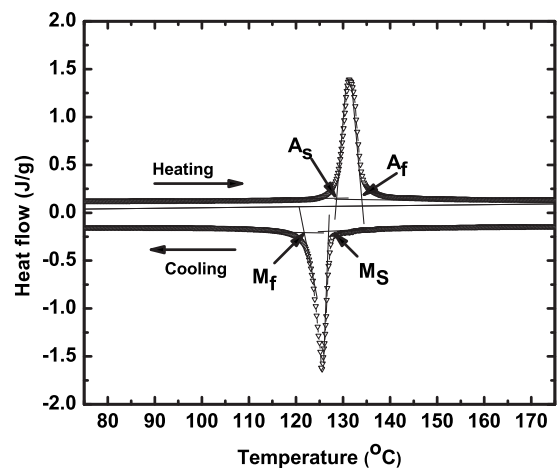


FIG. 1. Heat flow vs temperature in $\text{Ni}_{45}\text{Co}_5\text{Mn}_{40}\text{Sn}_{10}$.

^{a)}Electronic mail: james@umn.edu.

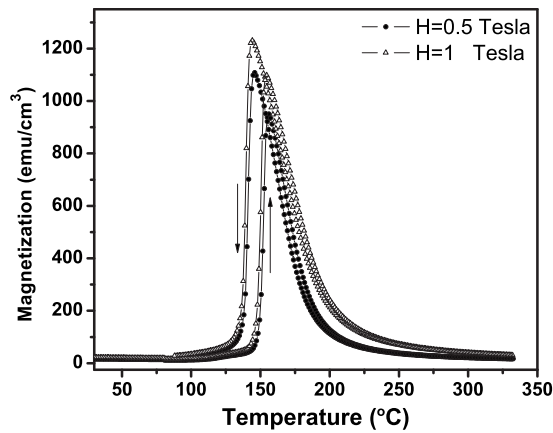


FIG. 2. Average magnetization vs temperature in $\text{Ni}_{45}\text{Co}_5\text{Mn}_{40}\text{Sn}_{10}$ at applied fields $H=0.5$ and 1.0 T.

full details will be reported in Ref. 14). The change in enthalpy ΔH is calculated to be 1.52 J/g. Using the formulas $\Delta S = \Delta H/T_0$ where $T_0 = 1/2(M_s + A_f)$ we calculate the change in entropy at the transformation to be 11.63 mJ/gK. These values are similar to those found in NiMnX ($X=\text{Sn}, \text{In}$).¹³

X-ray diffraction measurements on $\text{Ni}_{45}\text{Co}_5\text{Mn}_{40}\text{Sn}_{10}$ showed an austenite phase having a diffraction pattern consistent with a $L2_1$ Heusler-type structure with $a_0 = 0.5986$ nm (± 0.0001). The martensite phase exhibited a 5M modulated monoclinic structure with lattice parameters $a=0.4405$ nm, $b=0.5642$ nm, $c=2.1680$ nm, and $\beta=87.03^\circ$. By comparison, the martensite of the base alloy $\text{Ni}_{50}\text{Mn}_{40}\text{Sn}_{10}$ is reported as 7M monoclinic.¹³ These lattice parameters give a value $\lambda_2=1.0032$ (Refs. 15 and 16). This is quite close to 1. By way of comparison, in a recent study⁴ on a broad variety of alloys of the NiTiCuPd system prepared by combinatorial synthesis methods, most alloys having $|\lambda_2 - 1| < 0.0032$ exhibited thermal hysteresis in the range $0-10^\circ\text{C}$, whereas most alloys with $|\lambda_2 - 1| > 0.01$ exhibited hysteresis in the range than $30-70^\circ\text{C}$.

Figure 2 shows the thermomagnetization curves for $\text{Ni}_{45}\text{Co}_5\text{Mn}_{40}\text{Sn}_{10}$ obtained at the modest fields $H=0.5$ and 1 T. The magnetization is constant (nearly zero) at tempera-

tures below transformation, and there is an abrupt and remarkable change in magnetization at about 130°C . Already, a low temperature nonferromagnetic martensite and a high temperature ferromagnetic austenite is quite unusual. The hysteresis measured here is about 10°C , a little higher than that given by calorimetry. The discrepancy between these two data may have resulted from different specimen sizes, slightly different compositions, or different heating and cooling rates. There is no significant change in the transition temperatures and thermal hysteresis with applied field from $H=0.5$ to 1 T. However, one can estimate from the small displacement of the graphs the value 2.6°C per $T \pm 1^\circ\text{C}$ and this lies in the range allowed by the Clausius-Clapeyron equation based on the latent heat given above. At $H=1$ T, during reverse transformation from austenite to martensite, the magnetization of the sample drops from 1270 to 35 emu/cm^3 . This seems to be the largest change reported in this system, including measurements done at large applied fields. One can also see from Fig. 2 that the transformation temperatures are surprisingly high. Most previously studied alloys in the broad system $\text{NiCoMn}(\text{In}, \text{Sn}, \text{Sb})$ have transformation temperatures near or below room temperature.

Figure 3 shows the average magnetization versus field plots at different temperatures, 100 , 130 , 135 , and 145°C , labeled a, b, c, and d, respectively. Even relatively far below A_s at 100°C , the sample is not purely paramagnetic and the behavior suggests inhomogeneity. Just below transformation at 130°C the graph suggests ferromagnetism but with nearly zero remanence and coercivity. The absence of a clear saturation suggests either inhomogeneity or else a gradual ferrimagnetic to ferromagnetic transition. Figures 3(c) and 3(d) show the full development of the magnetic moment (1170 emu/cm^3). Both the unusually large moment at small applied field as well as the unusual softness are clear from these graphs. These graphs exhibit the highest moment and highest susceptibility we found among the alloys $\text{Ni}_{50-x}\text{Mn}_{50-x}\text{X}_x$ [$X=\text{Sn}, \text{In}, x=9, 10, 11, 12, 13$; $\text{Ni}_{50-x}\text{Co}_x\text{Mn}_{41}\text{Sn}_9$, $x=3, 5, 7, 9$; and $\text{Ni}_{50-x}\text{Co}_x\text{Mn}_{40}\text{Sn}_{10}$, $x=3, 5, 7, 9$ (see Ref. 14)].

These alloys include those with both higher and lower Co and Sn contents. In particular, we found tremendous

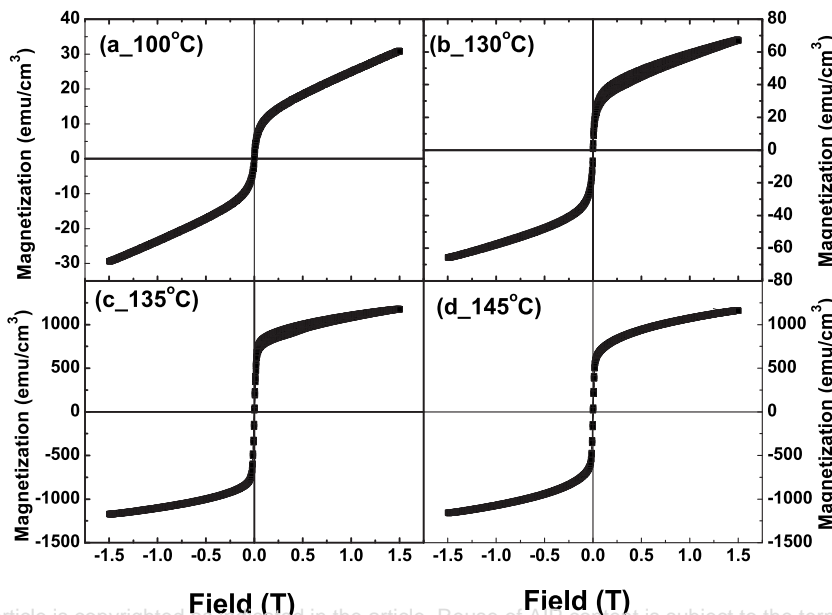


FIG. 3. Magnetization vs field in $\text{Ni}_{45}\text{Co}_5\text{Mn}_{40}\text{Sn}_{10}$ at temperatures 100 , 130 , 135 , and 145°C . Each measurement was preceded by heating to the Curie temperature.

sensitivity to compositional change. Starting with $\text{Ni}_{45}\text{Co}_5\text{Mn}_{40}\text{Sn}_{10}$, a decrease of 1% of Sn, substituting for Mn, results in a drop of the magnetic moment almost two orders of magnitude (to 25 emu/cm^3). Again starting with $\text{Ni}_{45}\text{Co}_5\text{Mn}_{40}\text{Sn}_{10}$, an increase of 2% of Co, substituting for Ni, results in a decrease in the magnetic moment by about a factor of about 2. A decrease of 2% of Co, substituted by Ni, results in a decrease in the magnetic moment by a factor of almost 4. The fact that these three unusual properties—high transformation temperature, large moment at small field, and $\lambda_2 \approx 1$ —occur simultaneously in $\text{Ni}_{45}\text{Co}_5\text{Mn}_{40}\text{Sn}_{10}$ could be coincidental, but invites speculation. There is not expected to be a correlation between these properties; the transition temperature is determined by the equality of free energies of the two phases, the magnetic moment is a bulk property determined from the electronic structure, and $\lambda_2 = 1$ is an interfacial property related to the coexistence of the two phases at nucleation. However, there are possible interesting scenarios where these properties could be related. For example, $\lambda_2 = 1$ allows an unstressed, untwinned interface between the two phases. If $\lambda_2 \neq 1$ then the growth of austenite is accompanied by finely twinned martensite. This condition is not only relevant to the nucleus, but also to the partly or fully transformed phase. When $\lambda_2 \neq 1$ the passage of austenite/martensite interfaces converting one phase to another leave in their wake a high density of twins. Optical micrographs of martensite in $\text{Ni}_{45}\text{Co}_5\text{Mn}_{40}\text{Sn}_{10}$ reveal a high density of martensite plates of width 5–10 μm . When $\lambda_2 \neq 1$ these are expected to be internally twinned at nanometer scale. In a recent high resolution TEM study¹⁷ of several alloys in the family $\text{Ti}_{50}\text{Ni}_{50-x}\text{Pd}_x$ with x chosen so that λ_2 approaches 1, there is considerable loss of fine structure at nanometer scale as $\lambda_2 \rightarrow 1$.

In this scenario alloys with $\lambda_2 \approx 1$, as in $\text{Ni}_{45}\text{Co}_5\text{Mn}_{40}\text{Sn}_{10}$, are expected to have many fewer nanoscale interfaces than nearby alloys. This would lower overall free energy of the martensite, and therefore raise the transformation temperature, as is seen. Some of this complexity could also, to a lesser extent, be inherited by the austenite during transformation, particularly if it has an inhomogeneous tweed structure. Such an inhomogeneous structure is in fact suggested by the slow saturation of the magnetization curves. It is also consistent with the overall observation that the exceptionally high magnetic moment occurs near the transformation temperature, dropping off to near zero in the

martensite but also dropping off quite rapidly also in the austenite. If so, a simpler austenite tweed associated with a $\lambda_2 = 1$ alloy may be able to exhibit increased alignment of magnetization and increased softness. These conjectures, which would imply an unexpected relation between $\lambda_2 = 1$ and magnetic properties, await elucidation by further careful studies.

This work was supported by Grant No. MURI W911NF-07-1-0410 administered by ARO. It also benefitted from the support of AFOSR GameChanger program GRT00008581/RF60012388 and MURI N000140610530 (ONR).

- ¹R. D. James and Z. Zhang, in *Magnetism and Structure in Functional Materials*, Springer Series in Materials Science, edited by A. Planes, L. Mañosa, and A. Saxena (Springer, New York, 2005), Vol. 79, p. 159.
- ²J. Cui, Y. S. Chu, O. O. Famodu, Y. Furuya, J. Hattrick-Simpers, R. D. James, A. Ludwig, S. Thienhaus, M. Wuttig, Z. Zhang, and I. Takeuchi, *Nature Mater.* **5**, 286 (2006).
- ³Z. Zhang, R. D. James, and S. Müller, *Acta Mater.* **57**, 4332 (2009).
- ⁴R. Zarnetta, R. Takahashi, M. L. Young, A. Savan, Y. Furuya, S. Thienhaus, B. Maaß, M. Rahim, J. Frenzel, H. Brunken, Y. S. Chu, V. Srivastava, R. D. James, I. Takeuchi, G. Eggeler, and A. Ludwig, *Adv. Funct. Mater.* **20**, 1 (2010).
- ⁵P. J. Webster, K. R. A. Ziebeck, S. L. Town, and M. S. Peak, *Philos. Mag. B* **49**, 295 (1984).
- ⁶Y. Sutou, N. Imano, T. Koeda, R. Omori, K. Kainuma, K. Ishida, and K. Oikawa, *Appl. Phys. Lett.* **85**, 4358 (2004).
- ⁷T. Krenke, E. Duman, M. Acet, E. F. Wasserman, X. Moya, L. Mañosa, and A. Planes, *Nature Mater.* **4**, 450 (2005).
- ⁸R. Kainuma, Y. Imano, W. Ito, H. Morito, Y. Sutou, K. Oikawa, A. Fujita, K. Ishida, S. Okamoto, O. Kitakami, and T. Kanomata, *Appl. Phys. Lett.* **88**, 192513 (2006).
- ⁹S. Y. Yu, L. Ma, G. D. Liu, Z. H. Liu, J. L. Chen, Z. X. Cao, G. H. Wu, B. Zhang, and X. X. Zhang, *Appl. Phys. Lett.* **90**, 242501 (2007).
- ¹⁰R. Kainuma, Y. Imano, W. Ito, Y. Sutou, H. Morito, S. Okamoto, O. Kitakami, K. Oikawa, A. Fujita, T. Kanomata, and K. Ishida, *Nature (London)* **439**, 957 (2006).
- ¹¹H. E. Karaca, I. Karaman, B. Basaran, Y. Ren, Y. I. Chumlyakov, and H. J. Maier, *Adv. Funct. Mater.* **19**, 983 (2009).
- ¹²T. Krenke, E. Duman, M. Acet, X. Moya, L. Mañosa, and A. Planes, *J. Appl. Phys.* **102**, 033903 (2007).
- ¹³T. Krenke, M. Acet, E. F. Wasserman, X. Moya, L. Mañosa, and A. Planes, *Phys. Rev. B* **72**, 014412 (2005).
- ¹⁴V. Srivastava and R. D. James, Hysteresis and multiferroism in cobalt substituted $\text{Ni}_{50}\text{Mn}_{40}\text{Sn}_{10}$ (to be published).
- ¹⁵K. F. Hane and T. W. Shield, *Acta Mater.* **47**, 2603 (1999).
- ¹⁶J. M. Ball and R. D. James, *Arch. Ration. Mech. Anal.* **100**, 13 (1987).
- ¹⁷R. Delville, S. Kasinathan, Z. Zhang, J. van Humbeek, R. D. James, and D. Schryvers, *Philos. Mag.* **90**, 177 (2010).